

Changes in the storage and sink of carbon dioxide in subsurface atmospheres controlled by climate-driven processes: the case of the Ojo Guareña karst system

Angel Fernandez-Cortes^{1,2} · Soledad Cuezva^{1,3} · Elena Garcia-Anton¹ · Miriam Alvarez-Gallego¹ · Concepcion Pla⁴ · David Benavente⁴ · Juan Carlos Cañaveras⁴ · Jose Maria Calaforra⁵ · David Paterson Matthey² · Sergio Sanchez-Moral¹

Received: 10 January 2015 / Accepted: 26 June 2015 / Published online: 8 July 2015
© Springer-Verlag Berlin Heidelberg 2015

Abstract A comprehensive environmental monitoring program was conducted in the Ojo Guareña cave system (Spain), one of the longest cave systems in Europe, to assess the magnitude of the spatiotemporal changes in carbon dioxide gas (CO₂) in the cave–soil–atmosphere profile. The key climate-driven processes involved in gas exchange, primarily gas diffusion and cave ventilation due to advective forces, were characterized. The spatial distributions of both processes were described through measurements of CO₂ and its carbon isotopic signal ($\delta^{13}\text{C}[\text{CO}_2]$) from exterior, soil and cave air samples analyzed by cavity ring-down spectroscopy (CRDS). The trigger mechanisms of air advection (temperature or air density differences or barometric imbalances) were controlled by continuous logging systems. Radon monitoring was also used to characterize the changing airflow that results in a predictable seasonal or daily pattern of CO₂ concentrations and its carbon isotopic signal. Large daily oscillations of CO₂ levels, ranging from 680 to 1900 ppm day⁻¹ on average, were registered during the daily oscillations of the exterior air temperature around the

cave air temperature. These daily variations in CO₂ concentration were unobservable once the outside air temperature was continuously below the cave temperature and a prevailing advective-renewal of cave air was established, such that the daily-averaged concentrations of CO₂ reached minimum values close to atmospheric background. The daily pulses of CO₂ and other tracer gases such as radon (²²²Rn) were smoothed in the inner cave locations, where fluctuation of both gases was primarily correlated with medium-term changes in air pressure. A pooled analysis of these data provided evidence that atmospheric air that is inhaled into dynamically ventilated caves can then return to the lower troposphere as CO₂-rich cave air.

Keywords CO₂ fluxes · CO₂ storage and evacuation · Karst terrains · Ojo Guareña karst system · Spain

Introduction

There is substantive evidence that CO₂ fluxes due to anthropogenic emissions do not coincide with those observed in the atmosphere, indicating in some early studies (Tans et al. 1990; Houghton et al. 1998) the existence of a significant missing terrestrial sink for this greenhouse gas. The region located between the soil surface and the groundwater table (unsaturated zone), which is mainly referred to as the vadose zone of karst terrains, is still an unaccounted terrestrial ecosystem in terms of CO₂ balances. Karst terrains form 15–20 % of the ice-free land surface (Engel 2011) and are an environment with a high capacity for gas exchange with the atmosphere and known mechanisms for sequestration of carbon as CO₂ (via carbonate dissolution and precipitation). While aspects of these processes are known, much detail still needs to be

✉ Angel Fernandez-Cortes
acortes@mncn.csic.es; Angel.Fernandez-Cortes@rhul.ac.uk

¹ Department of Geology, National Museum of Natural Sciences (MNCN-CSIC), 28006 Madrid, Spain

² Department of Earth Sciences, Royal Holloway, University of London, Egham, Surrey TW20 0EX, UK

³ Geomnia Natural Resources SLNE, 28003 Madrid, Spain

⁴ Department of Environment and Earth Sciences, University of Alicante, San Vicente del Raspeig, 03690 Alicante, Spain

⁵ Department of Biology and Geology, University of Almería, Ctra. Sacramento s/n, La Cañada De San Urbano, 04120 Almería, Spain

elucidated, such as the ventilation drivers and pathways, before carbon fluxes can be estimated. Therefore, the migration, temporal storage or consumption of CO₂ into subsurface atmospheres of the vadose zone have been traditionally neglected or underestimated in studies on net carbon balance in terrestrial ecosystems (Serrano-Ortiz et al. 2010). Previous models of carbon dioxide on a global scale assume that this sink is compensated by the source of oceanic CO₂ (Berner 1999), but some initial studies have highlighted the potential contribution of carbonate dissolution processes to this unknown sink (Liu and Zhao 2000; Gombert 2002; Liu et al. 2008).

The vadose zone of karst terrains may contain large amounts of gases occupying the air-filled cracks and voids of soil, bedrock or unconsolidated sediment (Benavente et al. 2010; Bourges et al. 2012). There is an abundant literature on the CO₂ efflux from soil to the atmosphere (Vargas et al. 2011, and references therein), but little is known about the downward flux into the subsoil and subsurface. However, it has been demonstrated that the shallow vadose environments below the soil show significant seasonal and even daily variations in CO₂ concentration, which involves the exchange of large amounts of CO₂(g) with the lower troposphere (Cuezva et al. 2011). Recent assessments of subterranean cavities have indicated that they act as sinks/reservoirs or net emitters/sources of CO₂ depending on the atmospheric conditions (Fernandez-Cortes et al. 2011; Garcia-Anton et al. 2014). The subsurface air may therefore play a key role as a sink or emitter of atmospheric carbon, but the pathways, mechanisms and fluxes of carbon in various gaseous forms (CO₂ or CH₄) among the atmosphere, soil and subsurface reservoirs are not yet well characterized.

Furthermore, the ongoing interest in belowground CO₂ capture and storage as one potential mitigation strategy to reduce anthropogenic CO₂ atmospheric emissions has underlined the need for more knowledge on the geologic storage capacity (Post et al. 2012; Nickerson and Risk 2013). Assessments are needed to ensure that there is no CO₂ leaking from storage formations and seeping out of the subterranean environment (Cohen et al. 2013). In this regard, a complete understanding of the medium- and short-term gaseous CO₂ transfer processes through the subterranean environment is essential.

Here, we contribute new data and an understanding of CO₂(g) variations at a small scale in a detailed field study of a shallow atmosphere belonging to a long subterranean system (Ojo Guareña karst, Spain). The overall aim of this study was to understand the specific constraints imposed by subterranean atmospheres (caves) located in the vadose zone of karst terrains for incorporating CO₂ dynamics into carbon-cycle models. To accomplish this objective, this study combined a multi-parameter monitoring of the cave–

soil–atmosphere (main climatic data and gas composition) with geochemical tracing using δ¹³C-CO₂ to assess the climate-driven fluctuations in CO₂(g) into the subsurface and its spatiotemporal pattern of exchange with the soil and atmosphere.

Study site

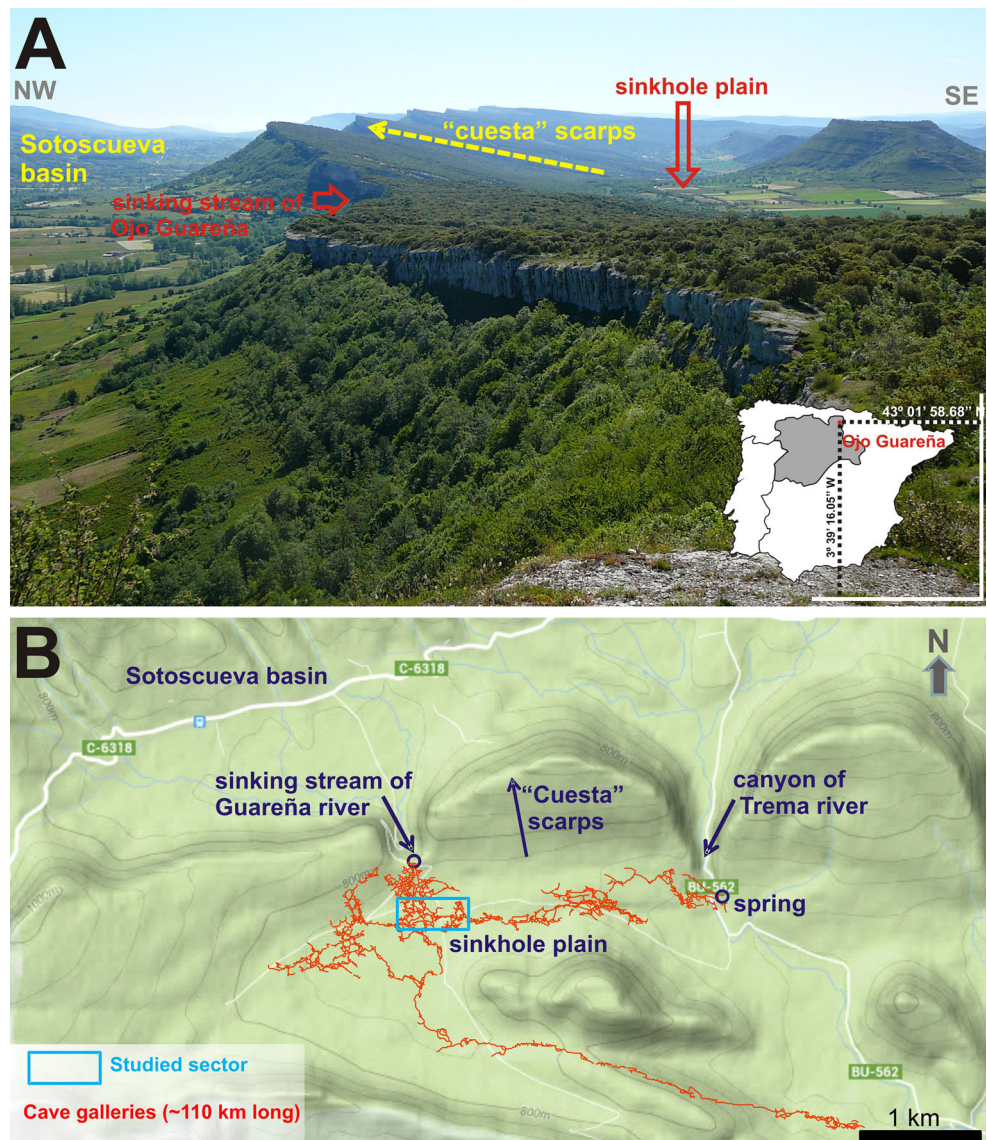
The study site is the Karst system of Ojo Guareña in the northern Spanish province of Burgos. In this geographic area, the climate is temperate without a dry season and with a temperate summer; the annual precipitation is approximately 640 mm, and the mean annual temperature is 11.9 °C (Fernandez-Cortes et al. 2015). Two main geomorphological units can be distinguished in this karst area in the Sotoscueva basin, containing a hydrological network at the surface and an elevated sinkhole plain with a landform on “cuesta” scarps related to a syncline with a sequence of Cretaceous limestones and marls (Fig. 1a).

In the opposite direction of the hydrological network (the Guareña and Trema rivers), in relation to the elevated “cuesta” scarps, is the geomorphological factor that controls the genesis of the subterranean system. In the boundary between both geomorphological units (Sotoscueva basin and “cuesta” scarps), there is a karstic canyon (Trema river) and also a sinking stream (Ojo Guareña). The latter is the main water input of runoff water that contributes to widening and developing the network of galleries. The subterranean water, and consequently the direction of the cave galleries, runs off to the catchment of the Trema River where several springs are located (Fig. 1b).

The Ojo Guareña cave system, one of the longest cave systems in Europe with over 100 km of development, is distributed over several overlapping levels composed of passages up to 10 m high and 20 m wide with three main entrances and several other minor cavities (Grupo Espeleológico Edelweiss 1986; Puch 1988; Camacho et al. 2006). In the sinkhole plain, we can find several entrances to the subterranean karst system, such as the Palomera doline and Dolencias sinkhole (Fig. 2a). Figure 2b shows a plan view of the study area. The present study was conducted in a sector some 3 km in length with three subsectors for continuous monitoring, Edelweiss, Gours Hojas and Museo Cera, and a network of 16 air-sampling points (Fig. 2). This sector represents only 2 % of the entire subterranean system.

The incoming flow of the Ojo Guareña sinking stream plays a key role in the environmental conditions of the studied galleries of the cave during the flooding season primarily after heavy and continuous rainfall that provokes the inundation of these galleries above the deeper levels where the Ojo Guareña sinking stream enters the cave. The inflow rate of water to the cave via the Ojo Guareña sinking

Fig. 1 Panoramic view (a) and relief map (b) of the karst system of Ojo Guareña. The location of the cave galleries is noted relative to the surface and the main geomorphological units. The photo from the upper panel was provided by the Environmental Service of Burgos belonging to the Regional Government of Castilla y León



stream ranges from $0.1 \text{ m}^3 \text{ s}^{-1}$ during the dry season to $0.65 \text{ m}^3 \text{ s}^{-1}$ in winter and spring (Grupo Espeleológico Edelweiss Grupo Espeleológico Edelweiss 1986). During extremely rainy events, the surface runoff waters are channeled into the Villamartin creek that ultimately runs into the cave through the waterfall located in the Dolencias sinkhole. Unfortunately, there are no data on the water flow entering the cave through the cascade of the Dolencias sinkhole.

Methods

A specific monitoring, sampling and analysis program was designed and implemented to obtain data on the CO_2 (g) contents and physical parameters of cave air via continuous logging by an installed network of sensors that

were spatially distributed and by means of spot air sampling by seasonal short surveys. The monitoring stations were installed in different locations according to several levels of microclimatic stability and the distance to the main entrances, specifically in the following galleries: Edelweiss, Gour Hojas and Museo Cera. Hourly data of the main cave air parameters were registered at these three cave locations, in addition to the exterior meteorological conditions located in the Dolencias doline (see Fig. 2). To date, a complete suite of time series has been registered from August 2013 to August 2014.

Each monitoring station consisted of a HOBO Pro v2 datalogger with built-in temperature and relative humidity sensors and a HOBO-U21 datalogger (Onset Computer Corporation, Bourne, MA, USA) accepting voltage and current inputs from a 4-channel multiplexer with 12-bit resolution. A set of special sensors were connected to this

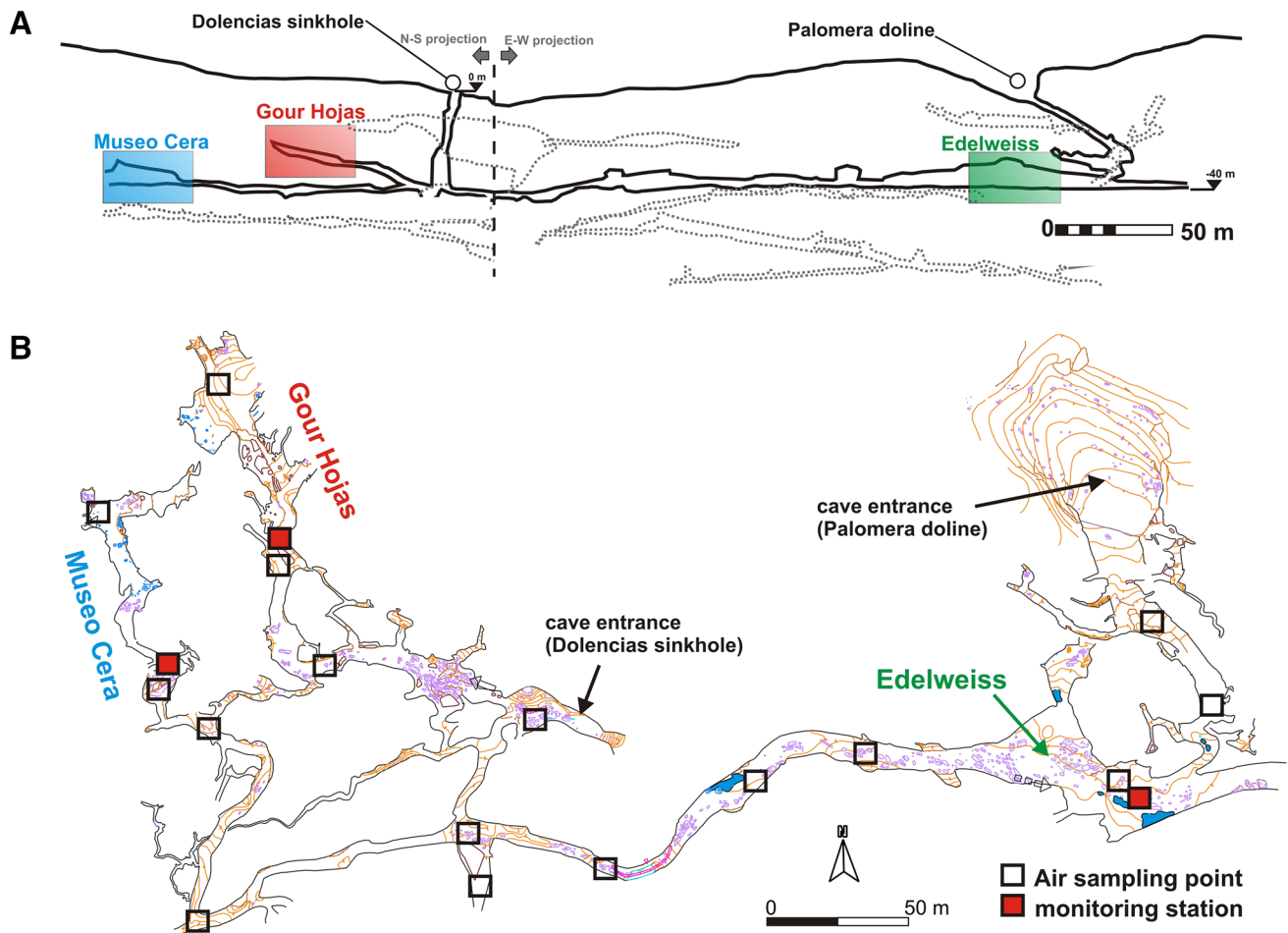


Fig. 2 **a** Detailed cross-sections of the cave galleries in relation to surface geomorphology and the main entrances to the subterranean system (*solid black line* represents the studied galleries; the ends of these galleries continue with the rest of the subterranean system,

which is not drawn; the *dotted lines* show the locations of other cave levels). Cross-sections modified from Grupo Espeleológico Edelweiss (1986). **b** Map of the cave sectors where spot air sampling and continuous monitoring were conducted

datalogger for the narrow range of measurements expected: air temperature (accuracy of ± 0.2 °C over 0–50 °C with a resolution of 0.02 °C at 25 °C), relative humidity (range from 0 to 100 % with a typical accuracy of ± 2.5 % from 10 to 90 % to a maximum of ± 3.5 % above 95 % and a resolution of 0.03 %) and barometric pressure (range of 660–1070 mbar with an accuracy of ± 3.0 mbar over the full pressure range at 25 °C and a resolution of 0.1 mbar). The outdoor weather station (HOBO U22) also included a tipping-bucket rain gauge for rainfall measurements up to 10 cm of rain per hour with an accuracy of ± 1 % up to 20 mm and a resolution of 0.2 mm.

The carbon dioxide concentration of cave air was registered with a K-33 ELG autonomous monitor (CO₂meter, Ormond Beach, FL, USA) based on non-dispersive infrared technology and a sampling method by gas diffusion. The measuring range was from 0 to 10,000 ppm, with an accuracy of ± 30 ppm or ± 3 % of the reading and a resolution of 1 ppm.

Ventilation of the cave atmosphere by advective forces was evaluated by monitoring its radon content (²²²Rn). Radon is a suitable tracer gas for cave ventilation (Kowalczyk and Froelich 2010) because of its half-life and inertness, i.e., it is not involved in the biogeochemical processes accounted for in the soil-subsurface profile. The ²²²Rn concentration of cave air was continuously registered (sampling interval of 30 min) using a Radim 5WP radon monitor (GT-Analytic KG, Innsbruck, Austria). This monitoring records the radon concentration of air by measuring the alpha-activity of the decay products of the conversion of radon, ²¹⁸Po and ²¹⁴Po collected from the detection hall on the surface of an Si-semiconductor detector by an electric field. The lowest activity detectable is 80 Bq/m³ for 1-h measurements with a statistical error equal to ± 20 %, and the maximum detectable activity is 150 KBq/m³.

Spot air sampling was conducted bimonthly in a predefined network of points that were spatially distributed in

the cave, soil and exterior during four short surveys (<3 h long). Exterior and soil air were sampled at fixed locations throughout the day and preferably during maximum (midday) and minimum photosynthetic activity (early morning). Soil air collection was conducted at sites located vertically above each cave using a steel tube with grooved sides at its end and inserted 20–50 cm near the bedrock–soil interface. Soil air was extracted using a micro-diaphragm gas pump (KNF Neuberger, Freiburg, Germany) at 3.1 l min^{-1} at atmospheric pressure. A portable air-compressor (AQUANIC s790) was run at 0.4 l min^{-1} for the cave air and atmosphere samples. Air samples were stored in 1-L Tedlar bags with lock valves. Bag samples were analyzed within 48 h of sampling for CO_2 concentrations and isotopic signals ($\delta^{13}\text{C}\text{CO}_2$) by a laser-based analyzer (Picarro G2101-i, California, USA) that employs cavity ring-down spectroscopy (Crosson 2008). Precisions of 200 and 10 ppb are guaranteed by the manufacturer for $^{12}\text{CO}_2$ and $^{13}\text{CO}_2$, respectively, over a wide operating range, with a resulting precision of less than 0.3 ‰ for $\delta^{13}\text{C}(\text{CO}_2)$ after 5 min of analysis. The maximum drift of $\delta^{13}\text{C}(\text{CO}_2)$ is less than 2.0 ‰ over 24 h at standard air pressure (peak-to-peak, 1-h average). Periodic tests were conducted to verify that the analyzer attained the above performance specifications (precision and drift) in accordance with the manufacturer's guidelines (test for 24 uninterrupted hours with the analyzer attached to a cylinder of compressed air with known CO_2 abundances).

Further information about the monitoring equipment and analytical techniques used in this study are detailed by Fernandez-Cortes et al. (2015).

A detailed multiparametric and spatially resolved monitoring of the main microclimatic parameters (temperature and relative humidity) in the underground air, the soil air and the external atmosphere was conducted during each specific survey, in tandem with the analysis of gas composition (CO_2 and $\delta^{13}\text{C}\text{CO}_2$). A set of high-accuracy probes (subjected to a standard and certified calibration) was used for this purpose: RTD PT100 sensor (C100, LUFFT), thermistor sensor (5611T, Hart Scientific), Hygropalm 1 (Rotronic) and a dual-wavelength infrared absorption sensor for CO_2 (SenseAir).

Results and discussion

CO_2 variations in cave air and ventilation regimes

Figure 3a, b shows the time series of cave air temperature related to the external weather conditions including air temperature and rainfall. During summer (from June to October) the cave air temperature is very stable according to a gradient of temperatures with lower values in the areas

close to entrances. The exterior temperature remains continuously below the cave air temperature during the winter period (from November to May). This provokes convective air circulation inside the cave and air exchange between the cave and the atmosphere (colder and denser) through the air inlet. Consequently, the cave air temperature decreases by up to $4 \text{ }^\circ\text{C}$, except in the most isolated areas (Museo Cera). The intense outside air inlet also provokes sharp decreases in relative humidity (up to 15 %) in the monitoring stations nearer to entrance (Edelweiss and Gour Hojas) (Fig. 3c).

The seasonal process of cave air renewal affects the gaseous composition of the cave atmosphere. Thus, the carbon dioxide concentration of the subterranean atmosphere has a stair-step pattern with strong shifts depending on the temperature relationship between the cave air and the atmosphere. Figure 4a shows the seasonal change in ventilation of the cave atmosphere, i.e., from summer to winter, which is reflected in the concentration of CO_2 (Fig. 4c) and ^{222}Rn (Fig. 4b). Thus, high summer and low autumn–winter levels were registered at each cave location during the monitoring period.

The daily CO_2 concentration reached atmospheric levels ($\sim 400 \text{ ppm}$), especially at locations near the main cave entrances and exposed to high ventilation rates (Edelweiss monitoring station, Fig. 2b). Advection is the mechanism that controls the CO_2 variations in the cave atmosphere, and it varies seasonally and daily, controlled by changes in meteorological conditions. The advective flux injects the outside air into the cave and extracts the subterranean CO_2 -enriched air. This process is triggered either by local temperature differences (thermal buoyancy due to different densities of warm and cold air), by intense wind or by a combination of both (Garcia-Anton et al. 2014). The advective influx of outside air during colder months also entails significant decreases in air temperature at those locations near cave entrances ($-2.25 \text{ }^\circ\text{C}$ in Gours Hojas and $-4 \text{ }^\circ\text{C}$ at the Edelweiss site), in addition to a depletion in the radon content of air at the most remote and isolated cave locations, e.g., the radon content of air from Museo Cera reached background levels of approximately 500 Bq m^{-3} (Fig. 4b).

The logging equipment also registered huge daily oscillations of CO_2 levels ranging 680–1900 ppm/day on average (from August to early October) (Fig. 4c), in accordance with two opposite patterns controlled by the outside air temperature: (1) CO_2 depletion (-47 to -166 ppm h^{-1} , on average) connected to sharp decreases in air temperature (-0.01 to $-0.06 \text{ }^\circ\text{C h}^{-1}$ on average, with maximums ranging from -0.15 to $-0.57 \text{ }^\circ\text{C h}^{-1}$) due to a nocturnal and early morning inlet of cold outside air and (2) an increase in the CO_2 concentration ($+58$ to $+182 \text{ ppm h}^{-1}$ on average) corresponding to a recovery of

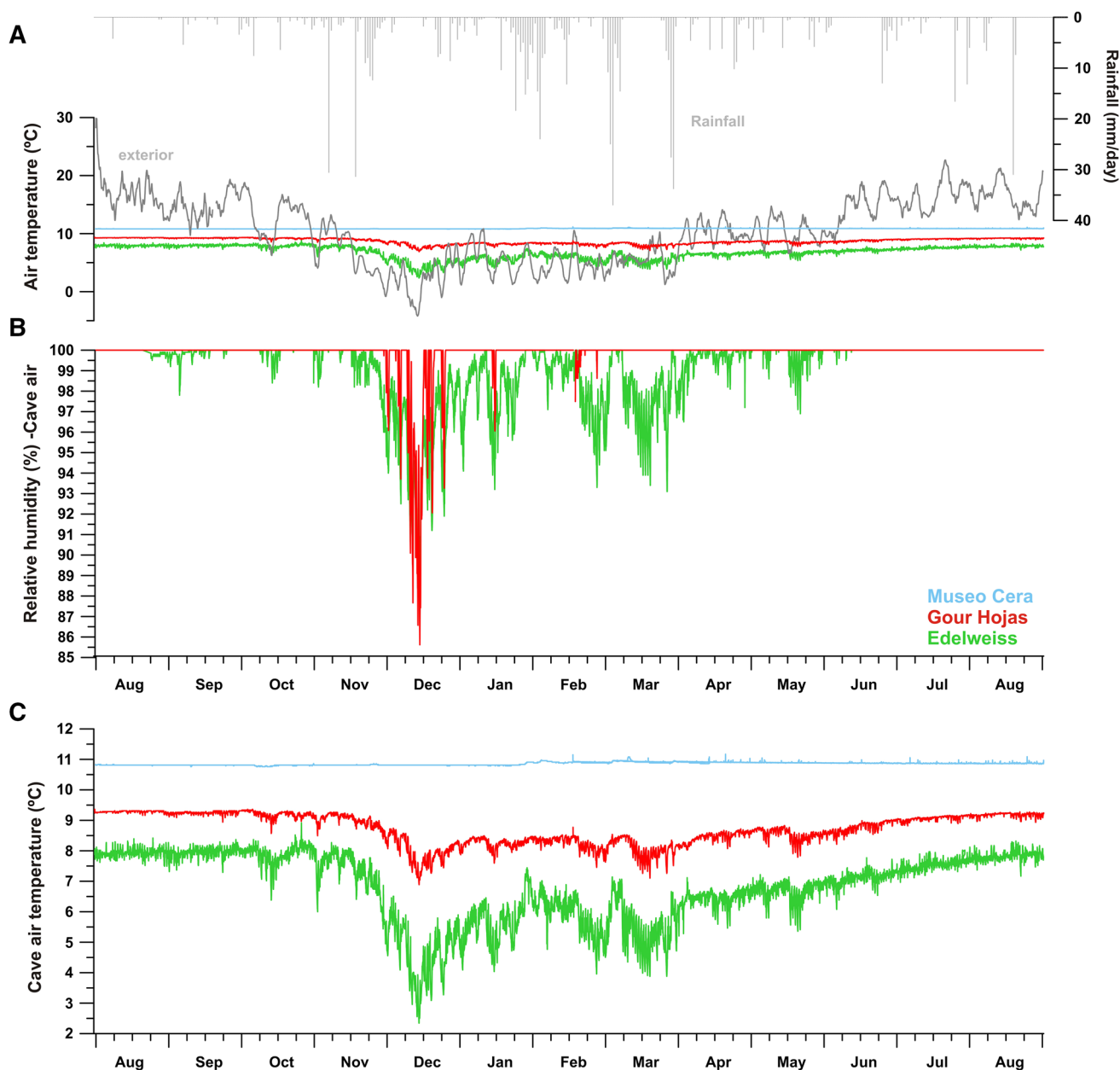


Fig. 3 Variations in the cave air temperature (**b**) and relative humidity (**c**) at three locations: Edelweiss, Gours Hojas and Museo Cera in relation to daily weather changes (temperature and rainfall)

(**a**) from August 2013 to August 2014. The relative humidity of the cave air at the Museo Cera site remained close to a steady state of saturation

cave air temperature during the daytime. These daily variations in the CO_2 content cease once the outside air temperature remains below the cave temperature and a stable mechanism of advective-renewal of cave air is established, such that the daily-averaged concentrations of CO_2 and ^{222}Rn reach minimum values close to 500 ppm and 700 Bq/m³, respectively.

The seasonal and daily fluctuations of gases as a function of temperature oscillation depend on the morphology of each cave sector and its location relative to exokarst.

Thus, the daily pulses of CO_2 as a function of external temperature variation are not observed in the inner cave locations (e.g., Museo Cera) where, conversely, variations in CO_2 are primarily controlled by the medium-term changes in air pressure (Fig. 5a). The natural fluctuations in the atmospheric pressure induce gas movement between the atmosphere and the subsurface, which is referred to as barometric pumping or atmospheric pumping (You et al. 2011, among other studies). The high pressure of cave air induces gas entrapment in Museo Cera, which is favored by

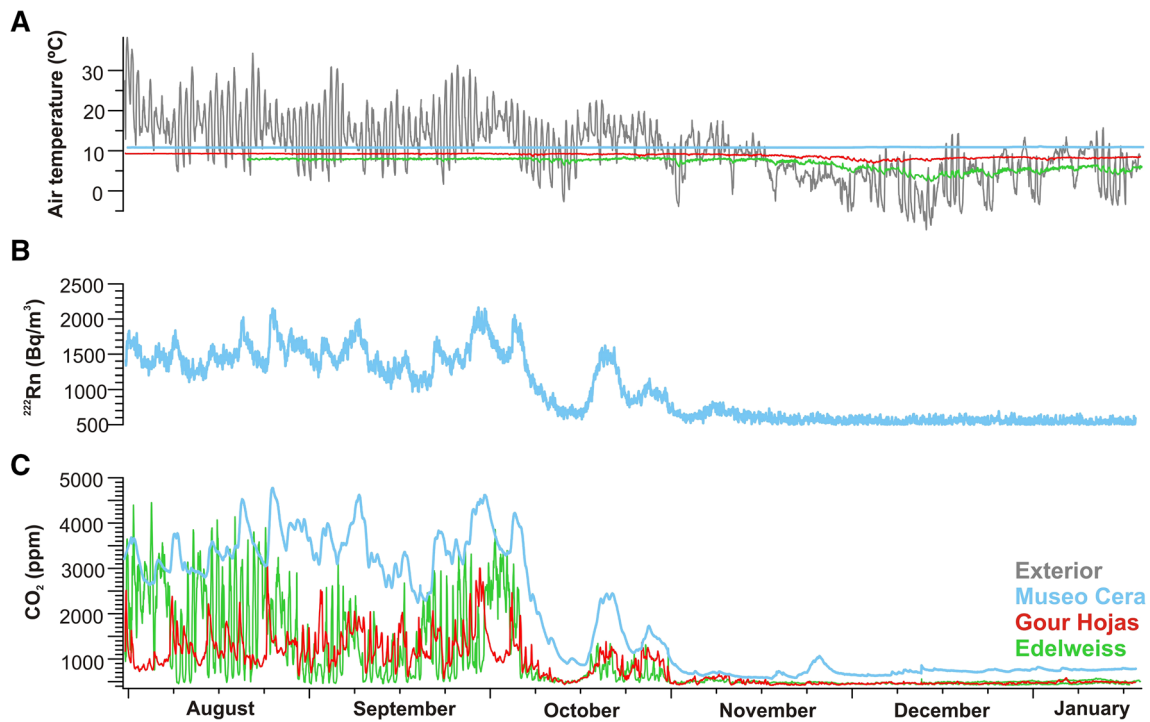


Fig. 4 Seasonal variation of the gaseous composition of the cave atmosphere: CO₂ (c) and ²²²Rn (b) in relation to the change in air temperature differences between the exterior and the cave environment from summer to winter (a)

a topographic effect of this gallery. Once the atmospheric pressure at the surface decreases, the pressure balance is re-established through breathing of CO₂-enriched air from Museo Cera and, consequently, as air with a lower CO₂ concentration from the surrounding cave sectors is forced into this gallery.

The fluctuations in atmospheric pressure at the surface and subsurface and its consequent influence on the subsurface airflow and gas transport are caused by two main reasons: (1) diurnal fluctuations due to gravitational effects (earth tides) and the warming and cooling of air caused by the daily alternation of solarization and (2) longer term fluctuations on the order of days to weeks due to weather and frontal systems as they move across the earth’s surface (Kuang et al. 2013). Figure 5a shows that the breathing pulses due to air pressure variations involves periodic but not daily changes in the CO₂ concentration in the isolated area of Museo Cera. The simultaneous fluctuations in cave air pressure and CO₂ concentration induced by variations in weather patterns are on the order of 5–10 mbar over periods of a few days. Outside air pressure variations are transmitted to the cave air, and an increase in cave air pressure causes the air masses located at isolated cave sites (e.g., cul-de-sac galleries as Museo Cera) to remain motionless. There is lesser air renewal under these aerodynamic conditions, and, therefore, the gases concentrations (CO₂ and ²²²Rn) tend to rise.

On the contrary, the daily renewal of cave air due to advective processes is triggered by inversion of the temperature gradient, which causes large changes in the CO₂ concentration in the areas closer to entrances, e.g., Edelweiss. The CO₂ concentration in this sector reaches the minimum values daily when the outside air temperature falls below the cave air temperature, primarily during night hours (Fig. 5b). These daily decreases in gas concentrations is even triggered before the exterior temperature is below the cave temperature, suggesting that colder and CO₂-depleted air masses from other cave locations can also be displaced to the Edelweiss gallery.

During periods of strong daily oscillations of CO₂ levels (Fig. 5b for the Edelweiss gallery), the sharp drops in the CO₂ level are followed by similar CO₂ increases during daylight hours. The increase in CO₂ concentration corresponds to an increase in air temperature difference between the exterior and the cave, but CO₂ maximums are reached with after a delay (5.6 h, on average) with respect to the maximum air temperature difference. In the absence of assessing the GHG contents and the isotopic signal δ¹³CO₂ by continuous real-time monitoring with CRDS techniques during several daily cycles, we hypothesize that a CO₂ concentration gradient between the deeper soil zones and karst–epikarst favors a downward CO₂ diffusive flow between both environments. The absence of ventilation results in a constant and progressive increase in the CO₂

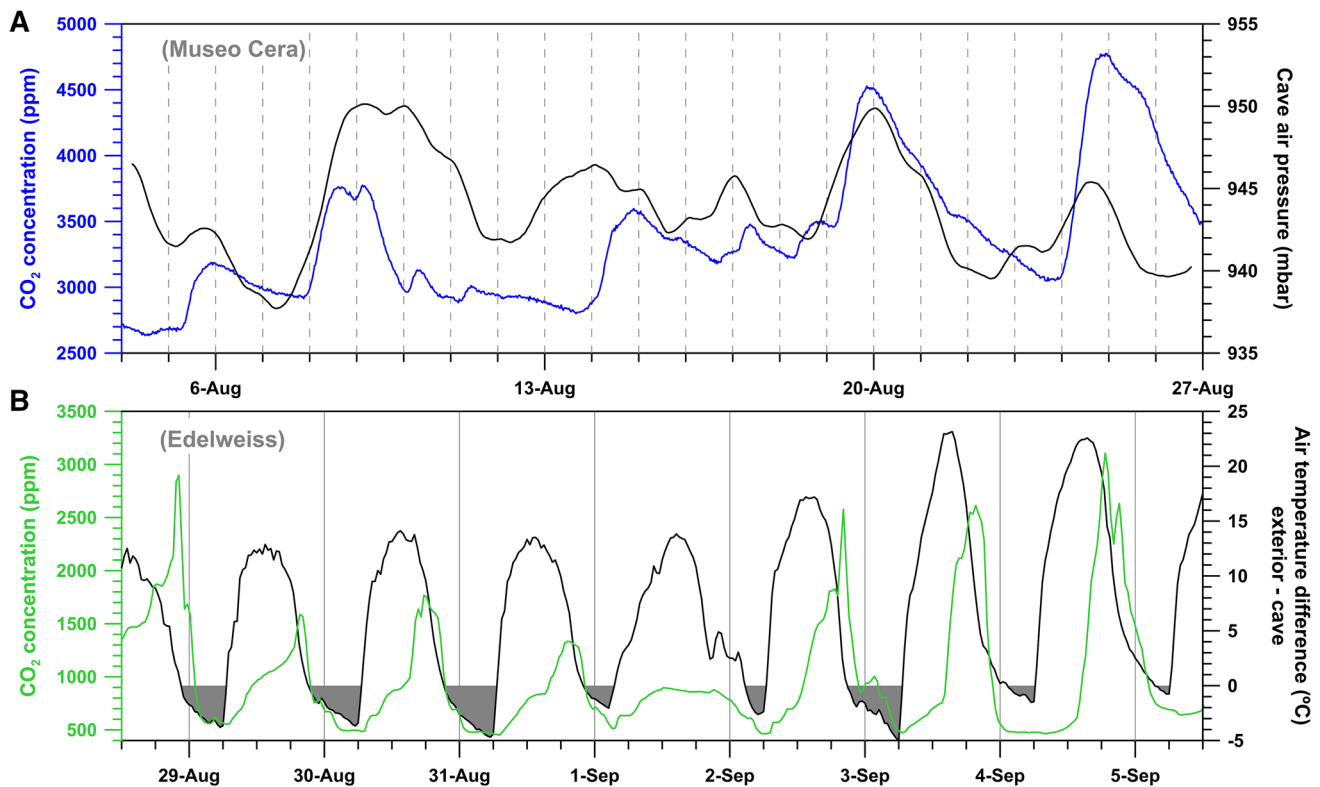


Fig. 5 Medium-term variations in carbon dioxide contents registered in Museo Cera as a function of cave air pressure changes (a) and daily pulses of CO₂ levels in Edelweiss primarily controlled by air temperature differences (exterior-cave) (b)

concentration in the cave from the surrounding epikarst (i.e., set of fissures, cracks and voids located above the galleries), as has been observed in other cavities, e.g., Altamira cave (Garcia-Anton et al. 2014).

The stable isotopic composition of gaseous carbon dioxide is a useful tool for understanding carbon cycling processes by determining the contributions of multiple carbon sources, as well as obtaining direct quantitative links to the sources of CO₂ and to the mechanisms that control gas transport and the transfer of carbon in the soil-cave system (Breecker et al. 2012) or in the atmosphere-soil-cave system (Garcia-Anton et al. 2014). In particular, the “Keeling plot” method for the analysis of the $\delta^{13}\text{C}\text{CO}_2$ isotopic signal assesses the processes that control an ecosystem’s isotopic discrimination (Pataki et al. 2003). This plot corresponds to a two-end mixing model that determines, by a linear regression approach, the carbon isotopic signal of the CO₂ sources of a specific ecosystem that contributed to increases in atmospheric CO₂. The y-intercept of the Keeling model corresponds to the carbon isotope composition of the integrated value of the CO₂ sources in the ecosystem.

For caves, the CO₂ concentration of underground air is broadly the result of mixing the background atmospheric CO₂ with soil-produced CO₂. In the case of Ojo Guareña,

the data were fitted with a Keeling model with a mean y-intercept value of -26.1‰ (Fig. 6). The soil holds four times as much carbon, on average, as does the cave atmosphere. Most soil carbon is derived from recent photosynthesis that takes carbon into root structures and into organic matter that can be carried deeper into bedrock storage and, subsequently, to the subsurface atmosphere. Therefore, soil respiration and carbonate precipitation act as sources of CO₂ that greatly increase the CO₂ molar fraction in the soil pore airspace, causing bidirectional diffusive transport between both the soil↔atmosphere and soil↔subsurface (subsoil and subterranean atmosphere). Thus, the CO₂ gas variations in the subsurface air are primarily controlled by gas diffusion from soil and air input from the outside atmosphere by advection. Accordingly, soil-produced CO₂ enters the subterranean atmosphere, increases the CO₂ concentration and reduces the isotopic signal ($\delta^{13}\text{C}\text{-CO}_2$). On the contrary, the direct input of outside air (without any soil influence) has a lower CO₂ concentration and heavier isotopic signal. Therefore, the CO₂-soil recharge by diffusion prevails during the end of summer, but the cave air becomes well mixed with the atmosphere during colder months (December–February).

As the distance of the cave air samples from the y-intercept of the Keeling models increases, there is greater

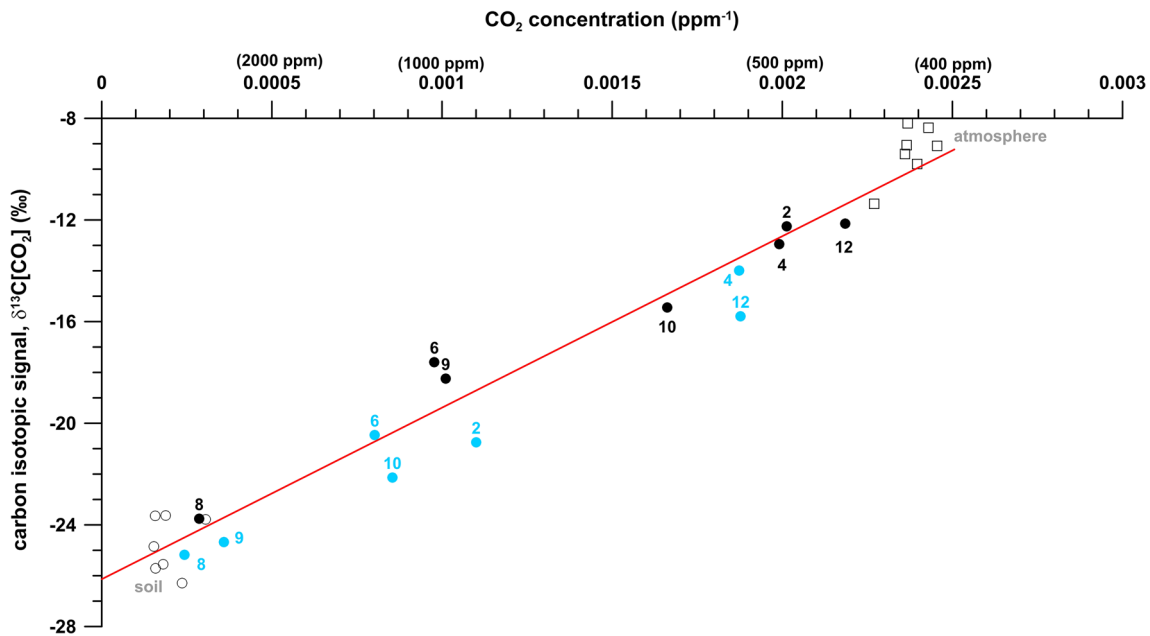


Fig. 6 Keeling model of CO₂ based on average values of CO₂ concentration and carbon isotope ratios registered during each bimonthly air sampling. A three-component mixture is distinguished: background atmosphere (*open squares*), soil air (*open circles*) and cave air (*solid circles*). *Black-solid circles* correspond to the average

data of cave air, and *blue-solid circles* correspond to air samples from Museo Cera. Numbers indicate the month in which the air sampling was conducted (1: January, ..., 12: December). Keeling model: $\delta C[CO_2] (\text{‰}) = 6749.4 \cdot [CO_2] (\text{ppm}^{-1}) - 26.1$, with $R^2 = 0.96$

ventilation and greater influence of the external atmosphere. Conversely, when CO₂ concentration is high and $\delta^{13}C_{CO_2}$ tends toward the y-intercept, the gas enters by diffusion and has a mainly edaphic origin. Consequently, air from more isolated galleries (e.g., Museo Cera) always has a higher CO₂ content and a $\delta^{13}C[CO_2]$ usually below -20 ‰ with respect to the other cave locations and considering the same air-sampling survey (Figs. 6, 7b, c), which points to a gas inlet with a primarily edaphic origin. Conversely, lower CO₂ contents and a $\delta^{13}C[CO_2]$ that tends to local atmospheric background (~9 ‰) denote a high air renewal rate of the cave atmosphere.

Air samplings were conducted at times of day with high ventilation rates, enabling the composition of a spatial distribution of the main cave sectors for storage or sinks of carbon dioxide. Figure 8 shows the spatial distribution of the average temperature, $\delta^{13}C[CO_2]$ and carbon dioxide concentration of the cave air during the studied period. The minimum temperature values near the Dolencias sinkhole are related to the presence of the stream of subterranean water to the other sectors of the cave and the occasional waterfall through this sinkhole during the wet season.

A prime example of an isolated sector is Museo Cera, which is topographically higher than the rest of cave sectors (Fig. 2). The lowest renewal of cave air was found in this eastern dead-end gallery, coinciding with the highest CO₂ (>2500 ppm) concentration, the lowest levels of $\delta^{13}C[CO_2]$

(<-23 ‰) and the maximum radon activity in the air, which indicates a lesser influence of aerodynamic processes. The atmosphere of this sector behaves as a warmer air mass entrapped in a void under a small overpressure. The thermal stratification of air creates a motionless trap of warm and less dense air that contributes to the CO₂ entrapment in Museo Cera (Fig. 7a), hindering the air exchange with the outer atmosphere. Microenvironmental data show that it operates as a motionless atmosphere that essentially does not take part in the daily aerodynamic process between the cave and the external atmosphere; it is, however, controlled by the following: (1) ‘breathing pulses’ due to air pressure imbalances (cave-exterior) that involve periodic but not daily changes in the direction of airflow and (2) seasonal (winter/summer) renewal of cave advective processes. The diffusive flux of soil-derived CO₂ prevails under these environmental conditions, so its isotopic signal $\delta^{13}C[CO_2]$ here reaches the minimum values compared to other cave locations (Fig. 7c).

Carbon fluxes and daily CO₂ balance after ventilation pulses

The discovery of frequent (daily), rapid (several hours) and large cycles of CO₂ recharge and ventilation in the Edelweiss gallery makes this subsurface location a hotspot of CO₂ sources from the vadose zone to the troposphere.

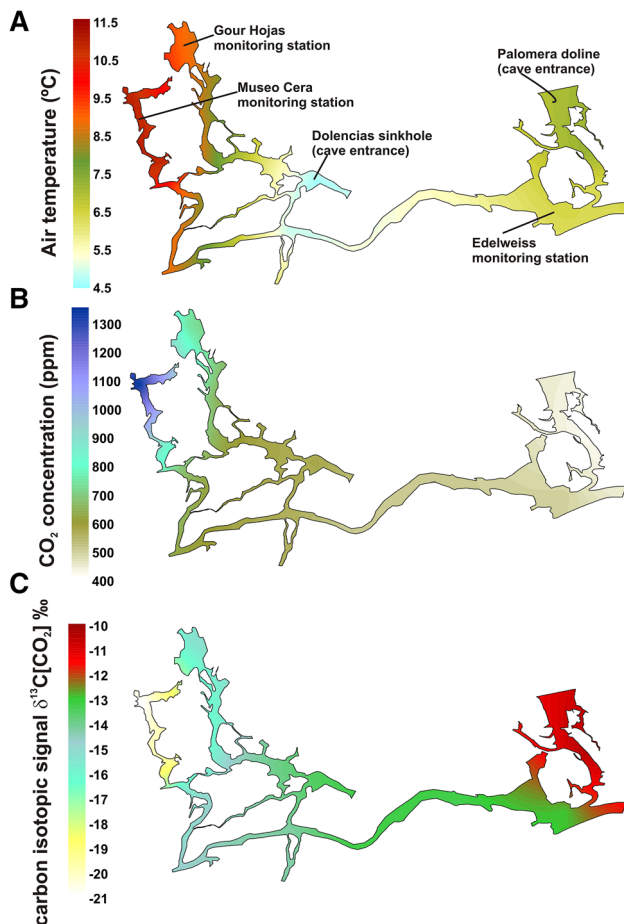


Fig. 7 Spatial distribution of air temperature (a), CO₂(g) concentration (b) and its carbon isotopic signal ($\delta^{13}\text{C}[\text{CO}_2]$) (c) and the temperature of main cave sectors into the Ojo Guareña karst system (see Fig. 2). Data for each contour map correspond to mean values from 7 bimonthly spot air samplings conducted from August 2013 to August-2014, showing the isolated areas and those with a prevailing air exchange with the exterior

The results summarized in Fig. 8a correspond to data records of daily variations in carbon concentrations in underground air from the Edelweiss gallery from early June to late October of 2014. The daily changes in the CO₂ concentration of cave air are primarily regarded as a response to changing cave ventilation during nighttime hours that are then modulated by gas diffusion from overlying soil and epikarst during daylight hours. At the Edelweiss gallery, the biotic CO₂ production and mass input of CO₂ from the degassing of drip water are considered negligible during the dry summer period because of the absence of both effective infiltration and active streams bringing organic matter into the cave from the outside.

During this complete summer period, the highest CO₂ concentrations in underground air of the Edelweiss gallery were registered every day between 19:00 and 21:00 h GMT (Greenwich Mean Time) after a continuous process of CO₂

diffusion from soil, reaching daily-averaged levels close to 2000 ppm. During nighttime, the temperature gradient is reversed, i.e., the outside air temperature is lower than the cave air temperature, which triggers a renewal process of underground air from the Edelweiss gallery through advective forces primarily along the Palomera doline. Consequently, the minimum concentrations were very often below 1000 ppm, and they were always reached during the early morning of the next day (between 8:00 and 9:00 h GMT), just at the end of the advective mixing of the cave air with exterior air. The drop in CO₂ between consecutive days was approximately 1350 ppm on average, but, during some daily cycles, the CO₂ levels decreased by 4250 ppm in just 12 h.

A mass-balance model can be constructed in terms of air advection between the Edelweiss gallery and the outside atmosphere. The CO₂ outgassing of the cave air during advection is primarily controlled by the air movement that produces the inflow of exterior air that is joined to an output of cave air. Therefore, during this stage of the day, the cave air is the resulting air mixture of the initial subterranean atmosphere (CO₂-background before the process) and a certain quantity of the exterior air input due to a volumetric movement. Considering a mass balance, the CO₂ concentration of the cave air (Edelweiss gallery) can be written as a time-dependent relation between the background component and the exterior component as follows:

$$[\text{CO}_2]_c(t) = [\text{CO}_2]_b + V_e(t) \times ([\text{CO}_2]_e - [\text{CO}_2]_b) \quad (1)$$

where $[\text{CO}_2]_c(t)$ is the daily (named as t) minimum concentration of CO₂ inside the cave (ppm) for each day (i.e., at the end of the advective period), $[\text{CO}_2]_b$ is the background (maximum) concentration of CO₂ (ppm) inside the cave on the previous day (i.e., beginning of the advective period), $[\text{CO}_2]_e$ is the concentration of CO₂ in the exterior atmosphere (approximately 430 ppm on average during the summer period in the area surrounding the cave entrance), and $V_e(t)$ is the total volume of exterior air input into the cave that is dependent on the time (relative volume) that results from the advective flux (or ventilation rate) between the exterior and the cave (Edelweiss gallery). Further details concerning the calculation of the mass balance of CO₂ in dynamically ventilated caves can be found in Garcia-Anton et al. (2014).

The mass balance of Eq. (1) allows us to quantify the ventilation rate (V_e) that affects the subterranean atmosphere and causes the CO₂ degassing in underground air. Thus, the total volume of the background component (V_b) and the total volume of the exterior component (V_e) can be expressed as relative volumes of the volume of the cave (V_c) as follows: $V_c = V_b + V_e = 1$. Therefore, the

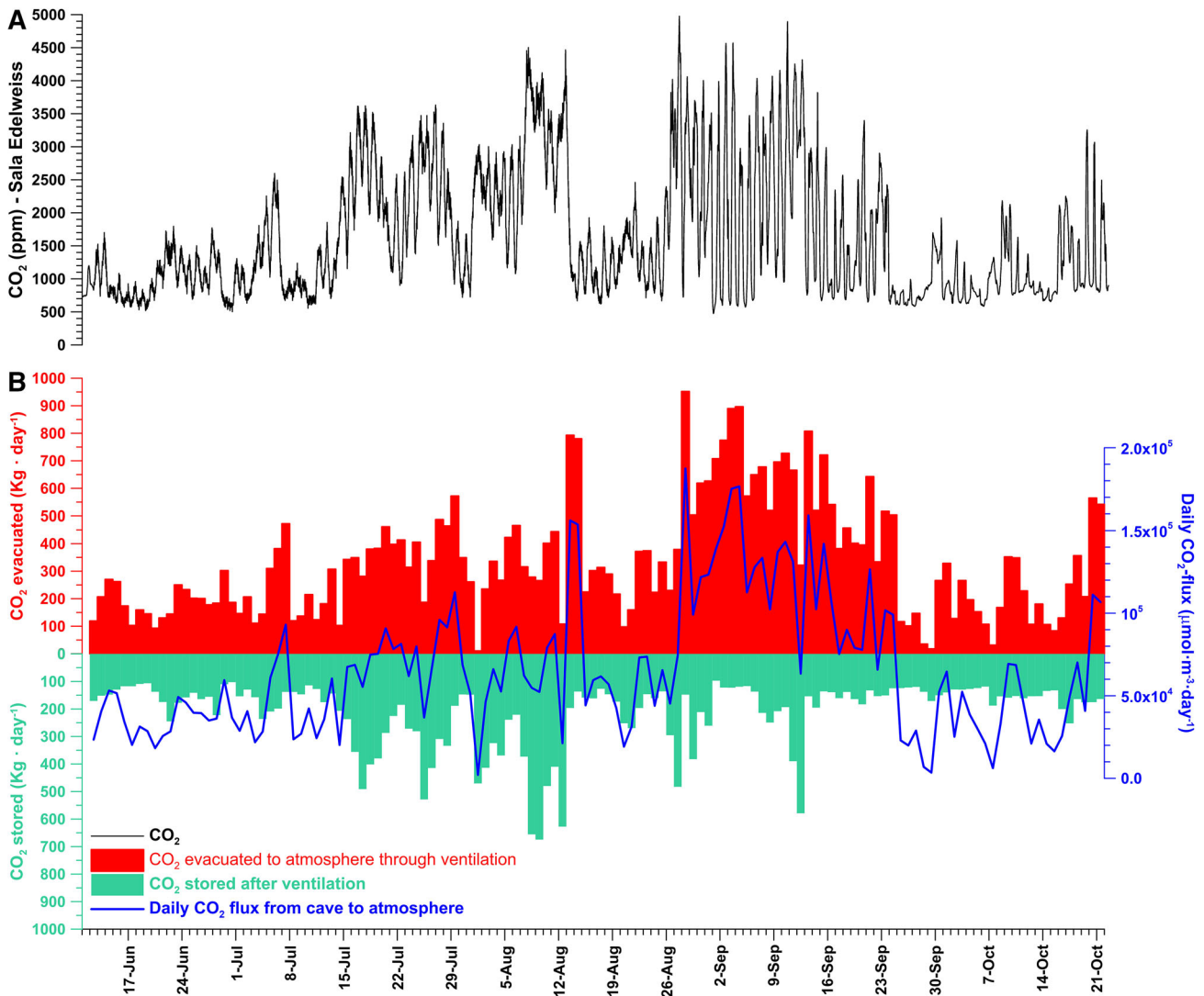


Fig. 8 **a** Daily variations in carbon concentrations in underground air from the Edelweiss gallery from early June to late October of 2014. **b** Balance between CO₂ outgassing and storage in the underground

after each daily pulse of ventilation and CO₂ flux (mmol day⁻¹ per cubic meter of air) from the gallery to the external atmosphere through ventilation

ventilation rate (V_e) is calculated as a function of the CO₂ concentration in cave air and in the exterior as follows:

$$V_e = \frac{([\text{CO}_2]_c - [\text{CO}_2]_b)}{([\text{CO}_2]_e - [\text{CO}_2]_b)} \quad (2)$$

Figure 8b shows the daily balance between CO₂ outgassing and storage in the underground air from the Edelweiss gallery after each daily pulse of ventilation (cave air renewal). It also includes the estimations of the daily CO₂ flux from the gallery to the external atmosphere through ventilation (in terms of μmol day⁻¹ per cubic meter of air). The net mass of CO₂ outgassed from the cave is controlled by ventilation and variations in CO₂. In general, as both ventilation and negative variations in CO₂ increase, CO₂ outgassing increases. The average net CO₂ outgassing from the Edelweiss gallery during summer (from June to October) was 7600 mol day⁻¹

(approximately 335 kg day⁻¹) considering a volume of the Edelweiss gallery of approximately 115.4 10³ m³, which is in turn connected with other galleries of the subterranean system. These data for outgassing fluxes of CO₂ are two orders of magnitude higher than the estimations for other caves, e.g., 120 mol day⁻¹ on average for the Hollow Ride cave (Kowalczk and Froelich 2010) or 2.34 to 11.71 kg day⁻¹ for Grotta di Ernesto (Frisia et al. 2011). These differences highlight the remarkable roles of the Edelweiss gallery and, the Ojo Guareña system in general, as both reservoir and, mainly, daily emitter with respect to other dynamically ventilated caves.

The advective flux between the exterior and the Edelweiss gallery provokes a daily renewal of the underground air mass from Edelweiss of approximately 67 % on average. The amount of CO₂ stored at the end of each daily

pulse of ventilation, $[\text{CO}_2]_s(t)$, corresponds to a mixture of air that results from the partial input into the cave of exterior air and the remaining CO_2 from underground air that is not evacuated as follows:

$$[\text{CO}_2]_s(t) = V_e(t) \times [\text{CO}_2]_e + V_b(t) \cdot [\text{CO}_2]_b. \quad (3)$$

The average net CO_2 stored in the mass of air from the Edelweiss gallery after ventilation was approximately $4800 \text{ mol day}^{-1}$ (212 kg day^{-1}) during summer.

On a daily average, the Edelweiss gallery clearly acts as a net emitter of CO_2 (i.e., it is able to emit more CO_2 than it stores) once the underground air is CO_2 -enriched during the previous night hours, primarily through gas diffusion from the soil and epikarst. Finally, a carbon imbalance was observed in the CO_2 molar fractions and masses by considering the entire summer season. In seasonal computing on a global scale, the CO_2 balance into the air from the Edelweiss gallery resulted in an evacuation of $1011 \cdot 10^3 \text{ mol}$ (44.5 T) of CO_2 to the outside atmosphere through ventilation during a summer period of 133 days.

Up-scaling: highly ventilated subterranean atmospheres as CO_2 emitters with significance in regional and global CO_2 budgets on different timescales

The phenomenon described here may thus be relevant on a global scale. However, there are not yet enough globally representative and tested data on presence and distribution of the subterranean atmospheres or caves, so extrapolation of any CO_2 sink/source model to a global scale still could entail much uncertainty. Nevertheless, in light of the above results, we propose a first up-scaling attempt in order to extrapolate to a global scale the CO_2 emission that has been described here for the subterranean atmosphere of Edelweiss gallery. The sequence of the applied calculations and the assumptions and constraints imposed were as follows:

1. A surficial Earth system analysis was performed with the aim of assessing potential subterranean hotspots for atmospheric CO_2 sinks or sources via ventilation processes. The global distribution of continental terrains suitable for hosting underground air pockets within their vadose zone but connected to the open atmosphere (mainly caves), was quantified. The voids and cavities filled with underground air are primarily due to the chemical dissolution of soluble layers of bedrock by variably acidic water, notably in carbonate rocks (limestone, dolomite or marble) and, to a lesser extent, evaporites rocks (mainly gypsum). Digital maps of the lithology of the continental surfaces were used to quantify the current global area of outcropping rock types. In particular, the present

surficial lithology for the nonglaciaded area of continents proposed by Durr et al. (2005) was used. The worldwide distribution of continental outcrops of carbonates rocks was also compared with results from other studies (Suchet et al. 2003; Ford and Williams 2007; Hollingsworth 2009). Lithologies linked to pseudokarst (Halliday 2004), i.e. lava tubes and piping caves in badlands terrains, among others, and other consolidated sedimentary rocks (according to Durr et al. 2005) with some portion of carbonate were not considered with the aims to simplify the calculation procedure.

2. Estimation of the area of rock outcrops for each lithological class that could potentially host subterranean atmospheres was performed using the areal coverage. Areal coverage is the fraction of the area of the cave field (outcrop) occupied by subterranean passages in a plan view (Klimchouk et al. 2000; Klimchouk 2004, 2006). The above studies assessed the variations of underground air volumes in the vadose zone resulting from speleogenesis, i.e., karst features such as cavities, in confined and unconfined settings through the analysis of typical morphometric parameters of a large and representative set of caves under the main soluble lithologies (limestone and gypsum). Areal coverage usually ranges from 28.4 % (gypsum caves) to 33.0 (limestone caves). In the case of carbonate rocks, karstification is a process that occurs in almost all outcrops worldwide (global area of $13\text{--}18 \cdot 10^6 \text{ km}^2$, Table 1) as karst settings are reported to cover from 12 to 25 % of the land surface of the Earth (White 1988; Ford and Williams 2007). Therefore, evaluation of the areal coverage is a suitable approach for estimating the fraction of the carbonate outcrop area under which it is feasible to find underground air masses.
3. The potential volume of soluble rock from the vadose zone capable of holding subterranean and interconnected air pockets was calculated for each lithological class at a global scale, by considering the previous global data on the dimensions of outcrops and their estimated areal coverage and depth.

The vadose zone is the portion of the subsurface above the groundwater table. In some places the vadose zone is absent, as is commonly observed where there are lakes and marshes, whereas in other areas, it is hundreds of meters thick, as is common in arid regions. The vadose zone may extend much deeper than the surficial soil layer and includes unsaturated rocks and alluvial materials down to depths of 100 m or more (Hopmans et al. 2005). However, it is more realistic to consider an average depth of 20 m as the maximum thickness of the karstified vadose zone

Table 1 Global estimates of CO₂ that is annually evacuated or stored for each lithological class favorable for hosting underground air in connection with the lower troposphere, according to the above sequence of up-scaling calculations

Lithological class	Global area of outcrops (×10 ⁶ km ²)	References	Estimated area of rock outcrops occupied by subterranean atmospheres (×10 ⁶ km ²)	Potential volume of soluble rock capable of holding subterranean air pockets (×10 ¹² m ³)	Estimated volume of subterranean air (×10 ¹² m ³)	Estimated amount of CO ₂ evacuated from subterranean atmospheres (Pg year ⁻¹)	Estimated amount of CO ₂ stored in subterranean atmospheres (Pg year ⁻¹)
Carbonate rocks	13.83	Dürr et al. (2005)	4.56	91.29	5.02	1.90	1.23
	16.71	Hollingsworth (2009)	5.51	110.28	6.07	2.29	1.48
	16.72	Ford and Williams (2007)	5.52	110.36	6.07	2.29	1.49
	18.03	Suchet et al. (2003)	5.95	119.00	6.54	2.47	0.01
Evaporites (mainly gypsum)	0.16	Dürr et al. (2005)	0.05	1.36	0.07	0.02	0.02
	0.24	Hollingsworth (2009)	0.07	2.01	0.03–0.10	0.02	0.01–0.02
Global average range Pg(CO ₂) year ⁻¹						2.26	1.46

where there is an active air exchange with the atmosphere via advective processes (i.e., bypassing the soil layer) at daily or seasonal scale. This threshold range agrees with the maximum depths at which underground air renewal is detected according to our cave monitoring results in other study sites (Fernandez-Cortes et al. 2015). The subterranean system of Ojo Guareña represents an exceptional case where air exchange reaches deeper locations (i.e., Edelweiss gallery is 40 m depth) due to the huge dimensions of galleries and cave entrances.

- The prospective volumes of underground air contained in the soluble rock from the vadose zone were inferred by considering the distinctive solution porosity for each lithological class. Solution (channel) porosity, or cave (macroscopic) porosity, is the fraction of the volume of a soluble rock block occupied by mapped cavities resulting from speleogenesis in the vadose zone of karst aquifers (Klimchouk 2006). It is the volume of the cave divided by the volume of the soluble rock block expressed as a percentage. Klimchouk (2006) calculated an average cave porosity of 5.5 % for limestone and 4.8 % for gypsum, but the value was an order of magnitude lower in the case of limestone aquifers under unconfined settings.
- We have considered an annual globally averaged abundance of atmospheric CO₂ of 390.5 ppm for the year 2011 (Hartmann et al. 2013) as the last published reference regarding the current global atmospheric CO₂ dry air mole fraction in the well-mixed

troposphere. Therefore, the estimate of the daily amount of atmospheric CO₂ that could be potentially stored in a single and standard subterranean atmosphere at global scale is approximately 757 mg m⁻³, considering a standard pressure (1 atm) and temperature (14.41 °C is the annual global combined land and ocean surface temperature for 2011 according to the National Oceanic and Atmospheric Administration (NOAA)—National Data Climate Center: <http://www.ncdc.noaa.gov/sotc/global/2011/13>).

The storage and ventilation of underground air at the Ojo Guareña cave was described in the previous section in terms of CO₂ abundance on different timescales (daily and seasonal) and for the particular geomorphological and climate settings of the Edelweiss gallery. As an initial approximation for the up-scaling procedure, we considered the above data registered for our study site and the annual globally averaged abundance of atmospheric CO₂. Thus, the daily-averaged mass of CO₂ (kg) evacuated and stored from a single subterranean system after each daily ventilation pulse during the season with intense cave air renewal (i.e., via advection and bypassing the soil) were estimated at 328 and 212 kg day⁻¹, respectively. In addition, the daily-averaged amount of atmospheric CO₂ that enters a subterranean atmosphere via advection was estimated at 51.9 kg day⁻¹, considering a daily renewal of the underground air mass of approximately 65 % on average.

Seasonal differences in meteorological conditions, with changes in rain events and in the duration of dry seasons,

can contribute to prominent changes in ventilation processes in the vadose zone, especially in the uppermost part connected to the atmosphere. The intensity and duration of ventilation processes in a subterranean atmosphere depend on a wide range of geomorphological and climate features of the local outcrop where it is located, including the bedrock and soil thicknesses, weather oscillations and the number and location of connections with the external atmosphere, among other factors. An average of 133 days per year was considered as the duration of the seasonal period with a prevailing daily ventilation of underground air via advective processes based on our monitoring results in the Ojo Guareña cave. This duration of the seasonal ventilation is also in agreement with records obtained at other subterranean sites (Fernandez-Cortes et al. 2015). The variation of the local air temperature is the parameter that best controls the air exchange between the connected vadose zone and the atmosphere, but this duration could be considered a representative average value of the worldwide duration of the opposite seasons in terms of air temperature conditions, regardless of the hemisphere considered.

Table 1 summarizes the annual estimates of CO₂ evacuated or stored for each lithological class favorable for hosting underground air in connection with the lower troposphere according to the above sequence of up-scaling calculations.

Subterranean atmospheres, mainly caves, can be considered as a temporal depot for CO₂ coming primarily from upper-layer soil diffusion or weathering. In scaling up our findings, we estimate the gas-phase storage in the terrestrial subsurface atmospheres (and potential ventilation) in the range of 1.46 Pg year⁻¹ by only considering the shallow subterranean atmosphere within the continental outcrops with porous rocks, particularly those that are susceptible to karstification. From this parameterization, we also estimate that the amount of subsurface-related CO₂ evacuated (via ventilation) could reach 2.26 Pg year⁻¹ on a global scale. These data have the same order of magnitude as previous estimates of the subterranean CO₂ pool and its potential ventilation (Serrano-Ortiz et al. 2010).

Conclusions

The caves from the vadose zone may contain large amounts of CO₂-rich air, some of which exhibits a direct connection to the open atmosphere. Within the complex set of biological, physical and chemical factors involved in the interstices of soil and bedrock, understanding the main climate-driven processes controlling CO₂ exchange in the entire atmosphere–soil–subsurface system is therefore key to assessing the carbon sequestration or release in these terrestrial ecosystems. Ultimately, this study characterizes

the periods of isolation, recharge and storage processes of gases in the subsurface environment of a long subterranean system, specifically the ventilation/venting processes and the resulting release/loss of stored gaseous CO₂ to the Earth's atmosphere.

This study involved spot sampling and measurement of gases in the atmosphere, soil and cave environments using cutting-edge spectroscopy techniques and instrumental systems for long-term monitoring of remote and hostile environments, such as subsurface (cave) and soil in karst terrains. In particular, the application of cavity ring-down spectroscopy allowed us to obtain high-accuracy measurements of CO₂ and its isotopic analysis ($\delta^{13}\text{CO}_2$) to improve our understanding of CO₂ exchange processes between cave environments, soils and the atmosphere. Comprehensive microclimatic monitoring of the exterior, soil and cave atmospheres conducted simultaneously with CO₂ tracking provided data for a full characterization of the time evolution and periodic variability of the microclimatic parameters, both individually and jointly in a spatial context (cave–soil–atmosphere). Overall, the spatiotemporal tracing of CO₂ and the continuous monitoring of microclimatic parameters of cave air conducted in this study are a suitable and reliable methodological approach to better understand the behavior and lifetime of the CO₂ in subsurface environments located in the vadose zone.

The spatiotemporal pattern of carbon dioxide described here provides evidence that atmospheric air that is inhaled into dynamically ventilated caves (e.g., Ojo Guareña) can then return to the lower troposphere as ¹²CO₂-rich cave air, even on short-term scales (daily). Some areas of long subterranean systems (e.g., Ojo Guareña) do not participate in the daily/seasonal renewal of cave air by convective forces, and they act as motionless atmospheres where gas accumulation and CO₂-soil diffusion prevail.

There is an intense gas exchange between the bulk of the atmosphere and large shallow caves such as Ojo Guareña, in particular at highly ventilated galleries such as Edelweiss. At this cave site, the underground air of this subterranean system shows significant seasonal and even daily variations in the CO₂ concentration, which involves the exchange of large amounts of CO₂(g) with the lower troposphere and its role as a depot and/or emitter. The amounts of carbon that might further be sequestered (CO₂) have a potentially significant impact on the regional atmospheric CO₂(g) budget because shallow caves may largely represent the volume of underground air that is distributed widely across continental ecosystems. In any case, this should be noticeable at a local scale by considering long subterranean systems such as Ojo Guareña karst.

By scaling up our findings, we estimated the subsurface-related CO₂ storage and evacuation on a global scale at 1.46 and 2.26 Pg year⁻¹, respectively. The CO₂ storage in

subterranean atmospheres could represent up to 56.2 % of the residual land CO₂ sink, i.e., the uptake of CO₂ in ecosystems excluding the effects of land use change. This terrestrial carbon sink has been estimated at 2.6 ± 1.2 Pg year⁻¹ for the last decade (2000–2009) according to the Fifth Assessment Report of the Intergovernmental Panel on Climate Change (Ciais et al. 2013). The estimate for the amount of CO₂ evacuated every year from subterranean atmospheres is approximately twice that of the CO₂ release from freshwater outgassing (lakes and rivers), and it could also represent 56.5 % of the annual growth rate of atmospheric CO₂ during the last decade (2000–2009), which has been estimated at 4.0 ± 0.2 Pg year⁻¹ (Ciais et al. 2013).

In accordance with these estimated data, the potential presence of hotspots in regions with subterranean atmospheres, e.g., karst areas, should be included when considering data from multiple atmospheric CO₂ inversion (top-down) models. In addition, future investigations should be focused on performing continuous monitoring of CO₂ in cave air and its carbon isotopic signal (δ¹³CO₂) in both well and poorly ventilated subterranean sites. The mechanisms and sources that affect the CO₂ contents of cave air should be identified to better understand the role of shallow vadose systems as a source/sink of this greenhouse gas.

Acknowledgments This research was funded by the Agreement between Fundación Patrimonio Natural (Regional Government of Castilla y León) and CSIC and by the Spanish Ministry of Economy and Competitiveness (MINECO) project CGL2013-43324-R and in collaboration with project CGL2011-25162-BTE. Funding was also provided by the People Programme (Marie Curie Actions—Intra-European Fellowships, call 2013) of the European Union’s Seventh Framework Programme (FP7/2007–2013) under REA grant agreement no. 624204, and the MINECO programme Torres Quevedo (PTQ 13-06296 and PTQ 12-05601).

References

Benavente J, Vadillo I, Carrasco F, Carrasco F, Soler A, Linan C, Moral F (2010) Air carbon dioxide contents in the vadose zone of a Mediterranean karst. *Vadose Zone J* 9:126–136. doi:10.2136/vzj2009.0027

Berner RA (1999) A new look at the long-term carbon cycle. *GSA Today* 9:1–6

Bourges F, Genthon P, Genty D, Mangin A, D’Hulst D et al (2012) Comment on carbon uptake by karsts in the Houzhai Basin, southwest China by Junhua Yan. *J Geophys Res Biogeosci* 117:G03006. doi:10.1029/2012JG001937

Breecker DO, Payne AE, Quade J, Banner JL, Ball CE, Meyer KW, Cowan BD (2012) The sources and sinks of CO₂ in caves under mixed woodland and grassland vegetation. *Geochim Cosmochim Acta* 96:230–246. doi:10.1016/j.gca.2012.08.023

Camacho AI, Valdecasas AG, Rodríguez J, Cuezva S, Lario J, Sanchez-Moral S (2006) Habitat constraints in epikarstic waters of an Iberian Peninsula cave system. *Ann Limnol Int J Limnol* 42:127–140. doi:10.1051/limn/2006009

Ciais P, Sabine C, Bala G, Bopp L, Brovkin V, Canadell J, Chhabra A, DeFries R, Galloway J, Heimann M, Jones C, Le Quéré C,

Myneni RB, Piao S, Thornton T (2013) Carbon and Other Biogeochemical Cycles. In: Stocker TF, Qin D, Plattner GK, Tignor M, Allen SK, Boschung J, Nauels A, Xia Y, Bex V, Midgley PM (eds) *Climate change 2013: the physical science basis* (chapter 6), Contribution of Working Group I to the Fifth Assessment Report of the Intergovernmental Panel on Climate Change. Cambridge University Press, Cambridge, United Kingdom and New York, pp 465–570

Cohen G, Loisy C, Laveuf C, Le Roux O, Delaplace P, Magnier C, Rouchon V, Garcia B, Cerepi A (2013) The CO₂-Vadose project: experimental study and modelling of CO₂ induced leakage and tracers associated in the carbonate vadose zone. *Int J Greenh Gas Control* 14:128–140. doi:10.1016/j.ijggc.2013.01.008

Crosson ER (2008) A cavity ring-down analyzer for measuring atmospheric levels of methane, carbon dioxide, and water vapor. *Appl Phys B Lasers Opt* 92:403–408. doi:10.1007/s00340-008-3135-y

Cuezva S, Fernandez-Cortes A, Benavente D, Serrano-Ortiz P, Kowalski AS, Sanchez-Moral S (2011) Short-term CO₂(g) exchange between a shallow karstic cavity and the external atmosphere during summer: role of the surface soil layer. *Atmos Environ* 45:1418–1427. doi:10.1016/j.atmosenv.2010.12.023

Durr HH, Meybeck M, Durr SH (2005) Lithologic composition of the Earth’s continental surfaces derived from a new digital map emphasizing riverine material transfer. *Glob Biogeochem Cycle* 19:GB4S10. doi:10.1029/2005GB002515

Engel AS (2011) Karst Ecosystems. In: Reitner J, Thiel V (eds) *Encyclopedia of geobiology, encyclopedia of earth sciences series 2011*. Springer, Dordrecht, pp 521–531

Fernandez-Cortes A, Sanchez-Moral S, Cuezva S, Benavente D, Abella R (2011) Characterization of trace gases’ fluctuations on a ‘low energy’ cave (Castañar de Ibor, Spain) using techniques of entropy of curves. *Int J Climatol* 31:127–143. doi:10.1002/joc.2057

Fernandez-Cortes A, Cuezva S, Alvarez-Gallego M, Garcia-Anton E, Pla C, Benavente D, Jurado V, Saiz-Jimenez C, Sanchez-Moral S (2015) The subsurface atmosphere a methane sink to be considered. *Nat Comm* 6:7003. doi:10.1038/ncomms8003

Ford DC, Williams PW (2007) *Karst Hydrology and Geomorphology*. Wiley, Chichester

Frisia S, Fairchild IJ, Fohlmeister J, Miorandi R, Spotl C, Borsato A (2011) Carbon mass-balance modelling and carbon isotope exchange processes in dynamic caves. *Geochim Cosmochim Acta* 75:380–400. doi:10.1016/j.gca.2010.10.021

Garcia-Anton E, Cuezva S, Fernandez-Cortes A, Benavente D, Sanchez-Moral S (2014) Main drivers of diffusive and advective processes of CO₂-gas exchange between a shallow vadose zone and the atmosphere. *Int. J. Greenh. Gas Control* 21:113–129. doi:10.1016/j.ijggc.2013.12.006

Gombert P (2002) Role of karstic dissolution in global carbon cycle. *Glob Planet Change* 33:177–184. doi:10.1016/S0921-8181(02)00069-3

Grupo Espeleológico Edelweiss (1986) Complejo kárstico de Ojo Guareña. In: Diputación Provincial de Burgos (ed) *Kaite*, vol 4-5. Diputación Provincial de Burgos, Burgos, Spain

Halliday WR (2004) Pseudokarst. In: Gunn J (ed) *Encyclopedia of Caves and Karst Science*. Fitzroy Dearborn, London, pp 1291–1301

Hartmann DL, Klein Tank AMG, Rusticucci M, Alexander LV, Brönnimann S, Charabi Y, Dentener FJ, Dlugokencky EJ, Easterling DR, Kaplan A, Soden BJ, Thorne PW, Wild M, Zhai PM (2013) *Observations: Atmosphere and Surface*. In: Stocker TF, Qin D, Plattner GK, Tignor M, Allen SK, Boschung J, Nauels A, Xia Y, Bex V, Midgley PM (eds) *Climate Change 2013: The Physical Science Basis* (chapter 2), Contribution of Working Group I to the Fifth Assessment Report of the

- Intergovernmental Panel on Climate Change. Cambridge University Press, NY, Cambridge, United Kingdom and New, pp 159–254
- Hollingsworth E (2009) Karst regions of the world (KROW)—Populating global karst datasets and generating maps to advance the understanding of karst occurrence and protection of karst species and habitats worldwide. MS Thesis in Geology. University of Arkansas
- Hopmans JW, van Genuchten, MTh (2005) Vadose zone: hydrological processes. In: Hillel D (ed) *Encyclopedia of Soil in the Environment*, Elsevier Ltd., pp: 209–216. doi:[10.1016/B0-12-348530-4/00434-3](https://doi.org/10.1016/B0-12-348530-4/00434-3)
- Houghton RA, Davidson EA, Woodwell GM (1998) Missing sink, feedbacks, and understanding the role of terrestrial ecosystems in the global carbon balance. *Glob Biogeochem Cycle* 12(1):25–34. doi:[10.1029/97GB02729](https://doi.org/10.1029/97GB02729)
- Klimchouk A (2006) Unconfined versus confined speleogenetic settings: variations of solution porosity. *Int. J. Speleol.* 35(1):19–24
- Klimchouk A (2004) Morphometry of caves. In: Gunn J (ed) *Encyclopedia of caves and karst science*. Fitzroy Dearborn, London, pp 1120–1125
- Klimchouk AB, Ford DC, Palmer AN, Dreybrodt W (eds) (2000) *Speleogenesis: Evolution of Karst Aquifers*. National Speleological Society, Huntsville
- Kowalczyk AJ, Froelich PN (2010) Cave air ventilation and CO₂ outgassing by radon-222 modeling: how fast do caves breathe? *Earth Planet Sci. Lett* 289:209–219. doi:[10.1016/j.epsl.2009.11.010](https://doi.org/10.1016/j.epsl.2009.11.010)
- Kuang X, Jiao JJ, Li H (2013) Review on airflow in unsaturated zones induced by natural forcings. *Water Resour Res* 49:6137–6165. doi:[10.1002/wrcr.20416](https://doi.org/10.1002/wrcr.20416)
- Liu Z, Zhao J (2000) Contribution of carbonate rock weathering to the atmospheric CO₂ sink. *Environ Geol* 39:1053–1058
- Liu Z, Dreybrodt W, Wang HJ (2008) A possible important CO₂ sink by the global water cycle. *Chin Sci Bull* 53(3):402–407. doi:[10.1007/s11434-008-0096-9](https://doi.org/10.1007/s11434-008-0096-9)
- Nickerson N, Risk D (2013) Using subsurface CO₂ concentrations and isotopologues to identify CO₂ seepage from CCS/CO₂-EOR sites: a signal-to-noise based analysis. *Int. J. Greenh. Gas Control* 14:239–246. doi:[10.1016/j.ijggc.2013.01.018](https://doi.org/10.1016/j.ijggc.2013.01.018)
- Pataki DE, Ehleringer JR, Flanagan LB, Yakir D, Bowling DR, Still CJ, Buchmann N, Kaplan JO, Berry JA (2003) The application and interpretation of Keeling plots in terrestrial carbon cycle research. *Glob. Biogeochem. Cycle* 17(1):1022. doi:[10.1029/2001GB001850](https://doi.org/10.1029/2001GB001850)
- Post WM, Izaurralde RC, West TO, Liebig MA, King AW (2012) Management opportunities for enhancing terrestrial carbon dioxide sinks. *Front Ecol Environ* 10:554–561. doi:[10.1890/120065](https://doi.org/10.1890/120065)
- Puch C (1998) *Grandes Cuevas y Simas de España*. Espeleo Club de Gracia, Barcelona
- Serrano-Ortiz P, Roland M, Sanchez-Moral S, Janssens IA, Domingo F, Godderis Y, Kowalski AS (2010) Hidden, abiotic CO₂ flows and gaseous reservoirs in the terrestrial carbon cycle: review and perspectives. *Agric For Meteorol* 150(3):321–329. doi:[10.1016/j.agrformet.2010.01.002](https://doi.org/10.1016/j.agrformet.2010.01.002)
- Suchet PA, Probst JL, Ludwig W (2003) Worldwide distribution of continental rock lithology: implications for the atmospheric/soil CO₂ uptake by continental weathering and alkalinity river transport to the oceans. *Glob Biogeochem Cycle* 17(2):1038. doi:[10.1029/2002GB001891](https://doi.org/10.1029/2002GB001891)
- Tans PP, Fung IY, Takahashi T (1990) Observational constraints on the global atmospheric CO₂ budget. *Science* 247:1431–1438. doi:[10.1126/science.247.4949.1431](https://doi.org/10.1126/science.247.4949.1431)
- Vargas R, Carbone MS, Reichstein M, Baldocchi DD (2011) Frontiers and challenges in soil respiration research: from measurements to model-data integration. *Biogeochemistry* 102(1–3):1–13. doi:[10.1007/s10533-010-9462-1](https://doi.org/10.1007/s10533-010-9462-1)
- White WB (1988) *Geomorphology and hydrology of karst terrains*. Oxford Univ. Press, Oxford
- You K, Zhan H, Li J (2011) Gas flow to a barometric pumping well in a multilayer unsaturated zone. *Water Resour Res* 47:W05522. doi:[10.1029/2010WR009411](https://doi.org/10.1029/2010WR009411)